Nonlinear excitations: Solitons

A. Mourachkine

Nanoscience Centre and the Cavendish Laboratory, University of Cambridge, 11 J. J. Thomson Avenue, Cambridge CB3 0FF, UK

The main purpose of this chapter is to present a brief introduction to nonlinear excitations, and to underline the soliton concept. This chapter is Chapter 5 in the book *High-Temperature Superconductivity: The Nonlinear Mechanism and Tunneling Measurements* (Kluwer Academic Publishers, Dordrecht, 2002), pages 101-142.

True laws of Nature cannot be linear. - Albert Einstein

One may wonder what this Chapter is doing in a book describing the phenomenon of superconductivity. The main purpose of this Chapter is to present a brief introduction to nonlinear excitations, and to underline the soliton concept. Acquaintance with nonlinear excitations is necessary since the Cooper pairs in high-T_c superconductors are pairs of soliton-like excitations. I am sure that, in 15 years or so, the presence of this Chapter in a book describing the phenomenon of superconductivity will be considered absolutely natural. There are excellent books devoted to the description of solitons and related phenomena; the reader who is interested knowing more on the soliton issues is referred to a few books (see Appendix).

I. INTRODUCTION

For a long time linear equations have been used for describing different phenomena. For example, Newton's, Maxwell's and Schrödinger's equations are linear, and they take into account only a linear response of a system to an external disturbance. However, the majority of real systems are *nonlinear*. Most of the theoretical models are still relying on a *linear* description, corrected as much as possible for nonlinearities which are treated as small perturbations. It is well known that such an approach can be absolutely wrong. The linear approach can sometimes miss completely some essential behaviors of the system.

Nonlinearity has to do with *thresholds*, with multistability, with hysteresis, with phenomena which are changed *qualitatively* as the excitations are changed.

In a linear system, the ultimate effect of the combined action of two different causes is merely the superposition of the effects of each cause taken individually. But in a nonlinear system adding two elementary actions to one another can induce dramatic new effects reflecting the onset of cooperativity between the constituent elements.

To understand *nonlinearity*, one should first understand *linearity*. Consider linear waves. In general, a *wave* may be defined as a progression through matter of a state
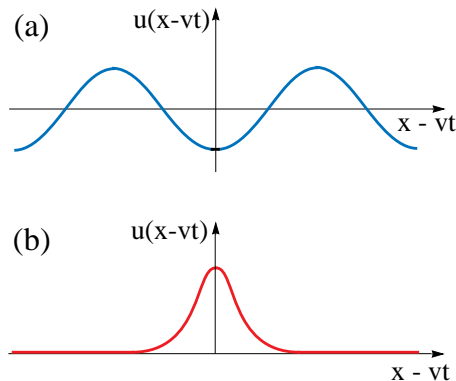

FIG. 1. Sketch of (a) a periodic linear wave, and (b) a solitary wave.

of motion. Characteristic properties of any linear wave are: (i) the shape and velocity of a linear wave are independent of its amplitude; (ii) the sum of two linear waves is also a linear wave; and (iii) small amplitude waves are linear. Figure 1a shows an example of a periodic linear wave. Large amplitude waves may become nonlinear.

The fate of a wave travelling in a medium is determined by properties of the medium. *Nonlinearity* results in the distortion of the shape of large amplitude waves, for example, in turbulence. However, there is another source of distortion—the *dispersion* of a wave. More than 100 years ago the mathematical equations describing *solitary waves* were solved, at which point it was recognized that the solitary wave, shown in Fig. 1b, may exist due to a precise balance between the effects of nonlinearity and dispersion. Nonlinearity tends to make the hill steeper (see Fig. 1b), while dispersion flattens it. The solitary wave lives "between" these two dangerous, destructive "forces." Thus, *the balance between nonlinearity and dispersion is responsible for the existence of the solitary waves*. As a consequence, the solitary waves are extremely robust.

Solitary waves or *solitons* cannot be described by using linear equations. Unlike ordinary waves which represent a spatial periodical repetition of elevations and hollows on a water surface, or condensations and rarefactions of a density, or deviations from a mean value of various physical quantities, solitons are single elevations, such

as thickenings etc., which propagate as a unique entity with a given velocity. The transformation and motion of solitons are described by nonlinear equations of mathematical physics.

The history of solitary waves or solitons is unique. The first *scientific* observation of the solitary wave was made by Russell in 1834 on the water surface. One of the first mathematical equations describing solitary waves was formulated in 1895. And only in 1965 were solitary waves fully understood! Moreover, many phenomena which were well known before 1965 turned out to be solitons! Only after 1965 was it realized that solitary waves on the water surface, nerve pulse, vortices, tornados and many others belong to the same category: they are all solitons! That is not all, the most striking property of solitons is that they behave like particles!

Mathematically, there is a difference between "solitons" and "solitary waves." *Solitons* are localized solutions of integrable equations, while *solitary waves* are localized solutions of non-integrable equations. Another characteristic feature of *solitons* is that they are solitary waves that are not deformed after collision with other solitons. Thus the variety of *solitary waves* is much wider than the variety of the "true" solitons. Some solitary waves, for example, vortices and tornados are hard to consider as *waves*. For this reason, they are sometimes called *soliton-like excitations*. To avoid this bulky expression we shall often use the term *soliton* in all cases. This is not dangerous when we are talking about general properties of soliton-like excitations.

II. RUSSELL'S DISCOVERY

The first observation of the solitary wave or soliton was made by John Scott Russell near Edinburgh (Scotland) in August 1834. He was observing a boat moving on a shallow channel and noticed that, when the boat suddenly stopped, the wave that it was pushing at its prow "rolled forward with great velocity, assuming the form of a large solitary elevation, a rounded, smooth and well defined heap of water which continued its course along the channel apparently without change of form or diminution of speed" [1]. He followed the wave along the channel for more than a mile. The shape of the solitary wave observed by Russell is similar to that in Fig. 1b.

Russell published the first report of this event in 1838. He called this solitary wave the *Wave of Translation.* A more detailed account of it and of successive experiments was published in his *Report on Waves* in 1844 [1].

Between 1834 and 1844, Russell performed numerous experiments in natural environments—on canals, rivers and lakes—as well as in his "laboratory," which was a specially designed small reservoir in his garden. In these studies, he found the following main properties of the solitary wave:

- An isolated solitary wave has a constant velocity and does not change its shape.

- The dependence of the velocity v on the canal depth h and the height of the wave, u, is given by the relation

$$v = \sqrt{g(h + u)},$$

where g is the gravity acceleration. This formula is valid for $u < h$.

- A high enough solitary wave decays into two or more smaller solitary waves. The new "born" solitary waves have different heights and, as a consequence, their velocities are different.

- There exist only solitary elevations (humps); solitary cavities (depressions) are never met.

In his report, Russell made a remark that "the great primary waves of translations cross each other without change of any kind in the same manner as the small oscillations produced on the surface of a pool by a falling stone". Researchers were very much puzzled by this striking phenomenon which was understood only 130 years later.

Russell was not only an exceptionally observant scientist and excellent experimenter but a first class theorist. However, the attitude to solitons of some most prominent theoretical experts at that time was quite different, and his colleagues neither saw its significance nor shared his enthusiasm. Moreover, there were even a few papers, including one written by Stokes, which concluded that the solitary wave cannot exist even in liquids with vanishing viscosity.

Unfortunately, such a situation happens often in science. As noted in Chapter 1, Abrikosov could not publish his famous paper during 5 years. The results described in the paper seemed to other physicists very strange. Even after 1957, when it was published, the results were accepted only after experimental proof of several predicted effects. Everyone who is really active in science experienced in his (her) lifetime the same attitude from other scientists. "I know how helpless an individual is against the spirit of his time," – Ludwig Boltzmann.

So, this was really a bad time for the solitary wave. Between 1844, when Russell's report was published, and 1965, fewer than two dozen papers relating to the solitary wave were published.

III. KORTEWEG–DE VRIES EQUATION

Fortunately, Russell lived long enough to see the solitary wave "acquitted" (he died in 1882). Boussinesq published a paper in 1871, in which he showed that Russell's

solitary wave may exist and approximately calculated its shape and velocity. The final verdict to the existence of the solitary wave was "announced" by Korteweg and de Vries in 1895. They reexamined all previous considerations and introduced a new equation for describing solitary waves that we now call the *Korteweg–de Vries* (KdV) equation [2].

Let $u(x, t)$ denote the height of the wave above the free surface at equilibrium, where t is the time and x is the coordinate along propagation of the solitary wave, the KdV equation is

$$\frac{\partial u}{\partial t} + \frac{3}{2h} u \frac{\partial u}{\partial x} + \frac{h^2}{6} \frac{\partial^3 u}{\partial x^3} = 0, \qquad (1)$$

where h is the depth of the water in the canal. This equation is written in a frame moving at the speed of long-wave linear disturbances of the surface. The exact solution of the KdV equation describing the soliton is

$$u(x, t) = u_0 \times sech^2 \left(\frac{x - vt}{\ell} \right), \qquad (2)$$

where u_0 is the initial height of the soliton; $v = \sqrt{gh}(1 + \frac{u_0}{2h})$, and 2ℓ is the "width" of the soliton and defined by the equation

$$S \equiv \frac{3}{4} \frac{u_0 \ell^2}{h^3} = 1. \qquad (3)$$

Equation (3) is the mathematical condition expressing the balance between the dispersion and nonlinearity effects in the soliton. Although the parameter S was known for decades, its role in soliton theory became clear fairly recently. If S is much larger than 1, nonlinearity effects will prevail (if the hump is smooth enough). They will strongly deform the hump and it will eventually break into several pieces that will probably give rise to several solitons. If $S < 1$, dispersion prevails, and the hump will gradually diffuse. For $S \approx 1$ the hump has a soliton-like shape and, if its velocity is close to the soliton velocity, it will slightly deform and gradually become the real soliton, described by the KdV equation.

The KdV equation played a crucial role in our times in resurrecting the soliton. For pure mathematicians, the history of solitons begins with the KdV equation. However, mathematicians did not fully realize the importance of the shallow water equation and neglected the KdV equation until the physicists returned it to life after 70 years of oblivion. In fact, Korteweg and de Vries themselves had no idea of the brilliant future awaiting their equation.

IV. NUMERICAL SIMULATIONS

With the appearance of computers, it became possible to simulate the behavior of nonlinear systems. Here
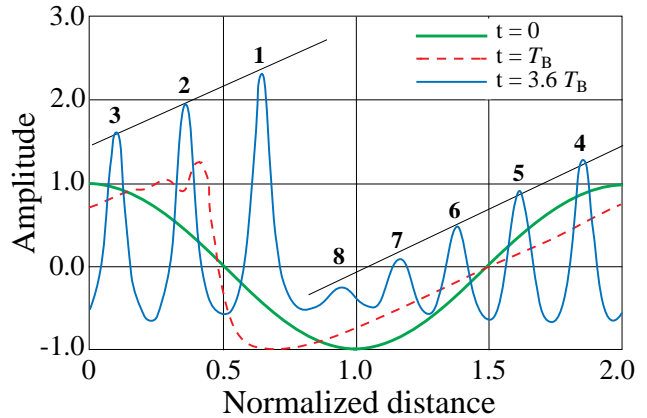

FIG. 2. The temporal development of the wave form $u(x)$ [4].

we shall consider two first computer "experiments": the first was performed by Fermi, Pasta and Ulam in 1955 [3], and the second ten years later—in 1965 by Zabusky and Kruskal [4]. Historically, both simulations were very important for understanding the behavior of nonlinear systems described by the KdV equation.

In 1955, Fermi, Pasta and Ulam (FPU) decided to investigate the behavior of a one-dimensional chain of 64 particles of mass m, bound by massless springs. They accounted for nonlinear forces by assuming that stretching the spring by $\Delta \ell$ generates the force $k\Delta \ell + \alpha(\Delta \ell)^2$. The nonlinear correction to Hooke's law, $\alpha(\Delta \ell)^2$, was assumed to be small as compared to the linear force, $k\Delta \ell$. Thus, the computer had to solve the following equations

$$m\ddot{u}_n = k(u_{n+1} - u_n) - k(u_n - u_{n-1}), \qquad (4)$$

with additional nonlinear terms in the right-hand side:

$$\alpha[(u_{n+1} - u_n)^2 - (u_n - u_{n-1})^2]. \qquad (5)$$

In the harmonic case ($\alpha = 0$), the energy stored initially in a given mode stays in that mode and the system does not approach thermal equilibrium. For $\alpha \neq 0$, Fermi, Pasta and Ulam started their simulation by exciting the lowest mode ($n = 1$), i.e. by choosing a non-localized initial condition having the shape of the plane wave with wavelength equal to the size of the system. At the beginning of the simulation, they observed that the energy slowly goes into other modes, so the modes 2, 3, 4, ... became gradually excited. But, to their surprise, after about 157 periods of the fundamental mode, almost all the energy was back in the lowest mode! After this recurrence time, the initial state was almost restored. This remarkable result, known as the FPU paradox, shows that introducing nonlinearity in a system does not guarantee an equipartition of energy. They also showed that nonlinear excitations can emerge not only from localized initial conditions but also from non-localized initial conditions or from thermal excitations.

When Kruskal and Zabusky heard of the results from the authors, they immediately started similar computer experiments: they considered movements of continuous nonlinear strings. After many attempts, they came to a striking conclusion: for small amplitudes, vibrations of the continuous FPU string are best described by the KdV equation!

The KdV equation describes a variety of nonlinear waves, and is suitable for small amplitude waves in materials with weak dispersion.

Zabusky and Kruskal solved the FPU paradox in 1965 because they plotted the displacements in *real space* instead of looking at the Fourier modes. Figure 2 shows the result of their simulations. They considered the evolution of a simple harmonic wave $u(0, x) = \cos(\pi x)$ shown by the green curve in Fig. 2. At some moment T_B ($= 1/\pi$), a characteristic step is formed (see the dashed red curve), which later at time $3.6T_B$ gives rise to a sequence of solitons, presented by the solid curve. In Fig. 2, the solitons are enumerated in descending order, the first having the largest amplitude. The first soliton is also the fastest one, and it is running down other solitons and eventually colliding with them. Shortly, after each collision, the solitons reappear virtually unaffected in size and shape. Thus, Zabusky and Kruskal proved that the KdV solitons are not changed in collisions, like rigid bodies. This property of solitary waves was mentioned in Russell's report. Zabusky and Kruskal also found that, as two solitons pass through each other, they accelerate. As a consequence, their trajectories deviate from straight lines, meaning that the solitons have particle-like properties. We shall discuss this remarkable feature in the next Section.

For the results of the simulation, shown in Fig. 2, the recurrence time T_R was found to be $T_R = 30.4T_B$. The FPU recurrence is simply a manifestation of the stability of the solitons. In fact, Zabusky and Kruskal studied waves in a plasma, which satisfy the KdV equation, and they coined the term *soliton*, 131 years after of its discovery.

V. PARTICLE-LIKE PROPERTIES

Intuitively, it is natural to consider solitary waves are *waves*. However, what Zabusky and Kruskal discovered in their computer simulation is that solitons behave like particles. Historically, neither Russell nor other scientists who studied the solitary wave more than a century after him noticed its striking resemblance to a particle. As mentioned above, Russell was aware of the particle-like property of two colliding solitary waves—after collision both solitary waves preserve their shapes and velocities. However, Russell didn't notice that, when the higher wave overtake the lower one, it appears that the first simply goes through the second and moves on ahead.
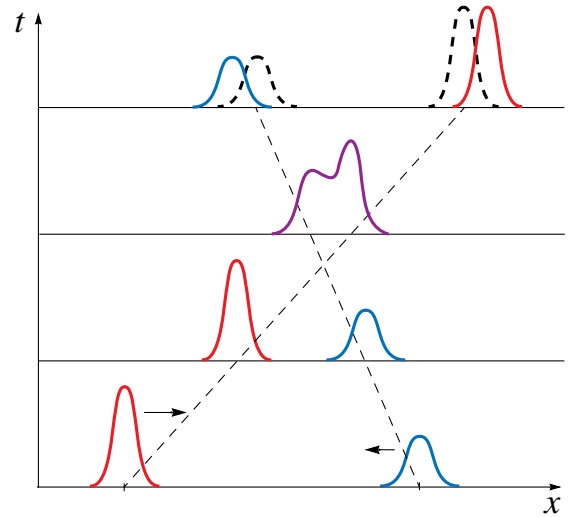

FIG. 3. A schematic representation of a collision between two solitary waves.

Russell obviously thought that this was true. In reality this is not the case. If Russell could have had a video camera, he would have seen that the process of the collision is somewhat different.

When the larger solitary wave touches the smaller solitary wave, which move slower, the larger one slows down and diminishes while the smaller one accelerates and increases. When the smaller wave becomes as large as the original one, the waves detach and the ex-smaller one, which now is higher and faster, goes forward while the ex-bigger one is now moving behind at lower speed. Figure 3 schematically shows a collision of two solitary waves. In Fig. 3, two solitary waves are depicted at different periods of time. The observable result of the collision, shown in Fig. 3, is that the larger wave appears to have **shifted** ahead of the position that it would have occupied in uniform motion (without the collision). While the smaller one appears correspondingly to have **shifted** backwards. Thus, the waves do not penetrate each other, but rather collide like tennis balls.

In order to understand this analogy, let us consider a collision of two tennis balls uniformly moving along the axis x. Suppose that the balls are identical, and they do not rotate. Let the velocities of the balls be v_1 and v_2. In the *center of mass system* of coordinates, which moves with the velocity $v = (v_1 - v_2)/2$, the balls have velocities v and $-v$. Figure 4 shows two balls at different periods of time. Assume that the balls touch each other at time t_1 and detach at time t_2. Between t_1 and t_2, the balls suffer first squeezing and then expanding. What is interesting that, at the end of the collision, thus at t_2, the centers of the balls are slightly ahead (behind) of the positions O_1' and O_2' which correspond to the balls positions if there were no collision. This sort of shift occurs if the time of the collision $(t_2 - t_1)$ is smaller than the "characteristic time" $2R/v$, where R is the radius of the balls.
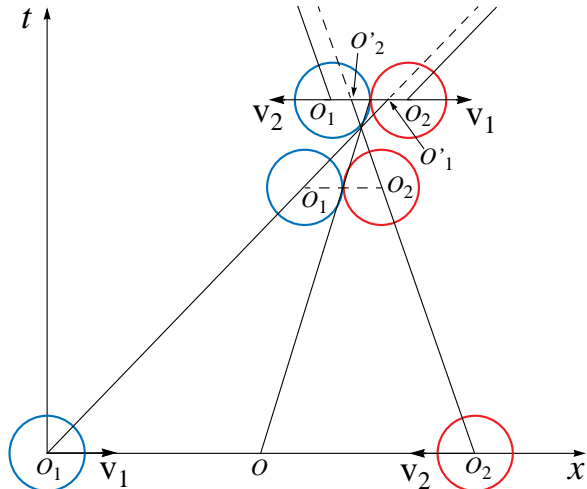
FIG. 4. A schematic representation of a collision between two tennis balls [5].

This experiment can be performed at home, if there is a fast-speed video camera. The question is why had no one noticed this striking particle-like property of the solitary wave? If Russell could not see this subtle effect because he didn't have proper equipment, it is more difficult to understand why experimenters using modern cinema equipment failed to observe the shift in 1952. The only reasonable explanation of this blindness of scientists is that everybody, including Russell, perceived the solitary wave as a *wave*. Even it was clear that this wave is very unusual, nobody could imagine regarding it as a particle. As soon as Zabusky and Kruskal found in their computer simulations that the solitary wave has much in common with particles, they cut off the word "wave" and gave the new name *soliton*, by analogy with electron, proton and other elementary particles.

VI. FRENKEL-KONTOROVA SOLITONS

To finish historical introduction to the soliton, let us consider one more event which is important in the history of the soliton.

All the examples of solitons, considered in the previous sections, are described by the KdV equation, and all these solitons belong to the same class of solitons: they are *nontopological*. The nontopological nature of these solitons can be easily understood because the system returns to its initial state after the passage of the wave. However, there are other types of solitons. The second group of solitons are so-called *topological* solitons, meaning that, after the passage of a topological soliton, the system is in a state which is different from its initial state. The topological stability can be explained by the analogy of the impossibility of untying a knot on an infinite rope without cutting it.
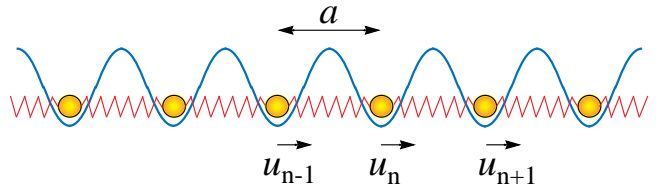

FIG. 5. The Frenkel-Kontorova model of one-dimensional atomic chain: a chain of atoms with linear coupling (springs) interacting with a periodic nonlinear substrate potential.

Frenkel and Kontorova theoretically predicted in 1939 topological solitons [6]. In fact, they found a special sort of a defect, called a *dislocation*, which exist in the crystalline structure of solids. The dislocations are not immobile—they can move inside the crystal.

Frenkel and Kontorova studied the simple possible model of a crystal which is shown in Fig. 5. In this one-dimensional model, atoms (black balls in Fig. 5) are distributed in a periodic sequence of hills and hollows which represent the substrate periodic potential. The balls rest at the bottom of each hollow because of the gravitational force. In Fig. 5, the springs which connect the balls represent the forces acting between atoms. It is evident that, in this model, a situation when one of the hollows is empty while all the balls are resting at the bottoms is impossible because of the springs. If one of the balls leaves a hollow (for example, n-th ball), the neighboring balls (n-1 and n+1) will be forced to follow. This creates an excitation which propagates further. The length of the excitation (or dislocation) is much larger than the interatomic distance, a. The long dislocation is mobile because small shifts of each atom do not require a noticeable energy supply. So, the dislocations in an ideal crystal freely move without changing its shape. However, if the crystal is imperfect, the dislocations will be attracted or repulsed by the defects. It is not difficult to understand that two dislocations repel each other, while dislocations are attracted by antidislocations.

The evolution of the dislocations and other topological solitons is described by the so-called *sine-Gordon* equation which we shall discuss in the next Section. The dislocation has the shape of a kink, shown in Fig. 6a. It has the *tanh*-like shape. The amplitude of the kink-soliton is independent of its velocity. As a consequence, topological solitons can be entirely static. The energy density of the kink-soliton is shown in Fig. 6b. In Fig. 6b, one can see that most of the energy of the kink, having the *sech*^{2} shape, is localized in its core (in the middle of the kink). Consequently, *the soliton is a localized packet of energy*. The energy of the soliton falls exponentially away from its center.
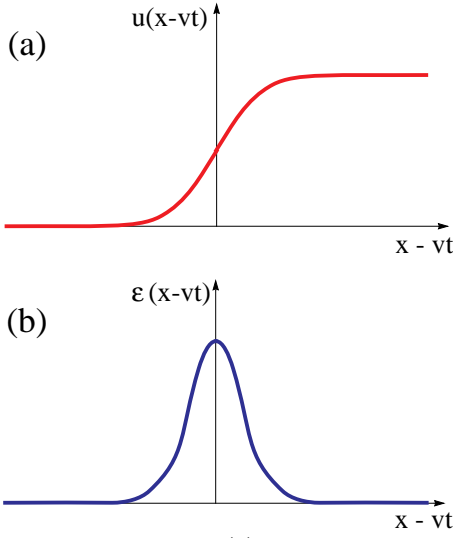
FIG. 6. Schematic plots of (a) a kink-soliton solution, and (b) the energy density of the kink-soliton.

VII. TOPOLOGICAL SOLITONS IN A CHAIN OF PENDULUMS

In order to understand better the nature of topological solitons, let us consider the propagation of a soliton in a chain of pendulums coupled by torsional springs. This mechanical transmission line is, probably, the simplest and one of the most efficient system for observing topological solitons and for studying their remarkable properties.

Figure 7 shows 21 pendulums, each pendulum being elastically connected to its neighbors by springs. If the first pendulum is displaced by a small angle θ, this disturbance propagates as a small amplitude linear wave from one pendulum to the next through the torsional coupling. As it moves along the chain, the small amplitude localized perturbation spreads over a larger and larger domain due to dispersive effects. The soliton is much more spectacular to observe. It is generated by moving the first pendulum by a full turn. This 2π rotation propagates along the whole pendulum chain and, even, reflects at a free end to come back unchanged.

The pendulum chain involves only simple mechanics and it is easy to write its equations of motion. Its energy is the sum of the rotational kinetic energy, the elastic energy of the torsional string connecting two pendulums, and the gravitational potential energy. Denoting by θ_n the angle of deviation of pendulum n from its vertical equilibrium position, by a the distance between pendulums along the axis, by m its mass and L the distance between the rotation axis and its center of mass, the expression of the energy is then
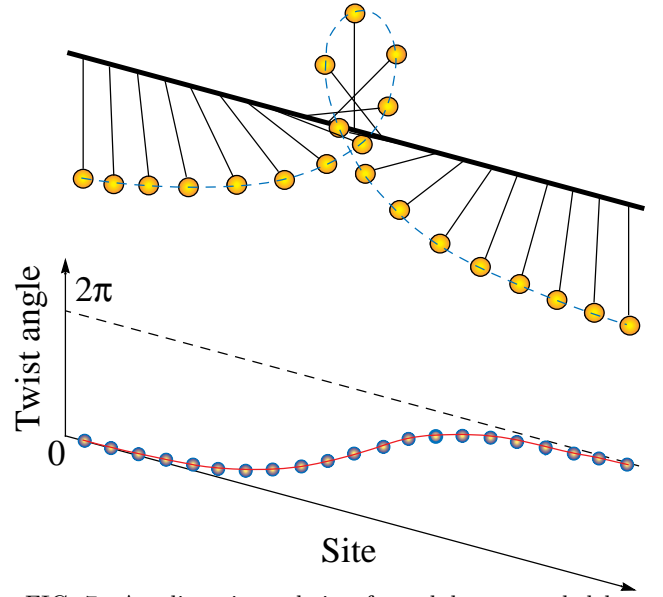

FIG. 7. A soliton in a chain of pendulums coupled by a torsional spring. The soliton is a 2π rotation. The lower figure shows the rotation angle of the pendulums as a function of their position along the chain.

$$H = \sum_n \frac{1}{2} I \left(\frac{d\theta_n}{dt} \right)^2 + \frac{1}{2}\beta(\theta_n - \theta_{n-1})^2 + mgL(1 - \cos\theta_n),$$
(6)

where I is the momentum of inertia of a pendulum around the axis, and β is the torsional coupling constant of the springs. The equations of motion which can be deduced from the hamiltonian are

$$\frac{d^2\theta_n}{dt^2} - \frac{c_0^2}{a^2}(\theta_{n+1} + \theta_{n-1} - 2\theta_n) + \omega_0^2 \sin\theta_n = 0, \quad (7)$$

where $\omega_0^2 = mgL/I$ and $c_0^2 = \beta a^2/I$.

This system of nonlinear differential equations, often called the *discrete sine-Gordon* equation, cannot be solved analytically. The common attitude in solving nonlinear equations is to *linearize* the equations. In our case, it can be done by replacing $\sin\theta_n$ by its small amplitude expression $\sin\theta_n \approx \theta_n$. Then the system of equations is easy to solve but *essential physics has been lost*. The linearized equations have no localized solutions and they have no chances to describe the soliton even approximately because $\theta_n = 2\pi$ is not a small angle. Thus, *by linearizing a set of nonlinear equations to get an approximate solution is not always a good idea*.

There is however another possibility to solve approximately this set of equations, while preserving their full nonlinearity, if the coupling between the pendulums is strong enough, i.e. $\beta \gg mgL$ (or $c_0^2/a^2 \gg \omega_0^2$). In this case, adjacent pendulums have similar motions and the discrete set of variables $\theta_n(t)$ can be replaced by a single function of two variables, $\theta(x, t)$ such that $\theta_n(t) = \theta(x =$
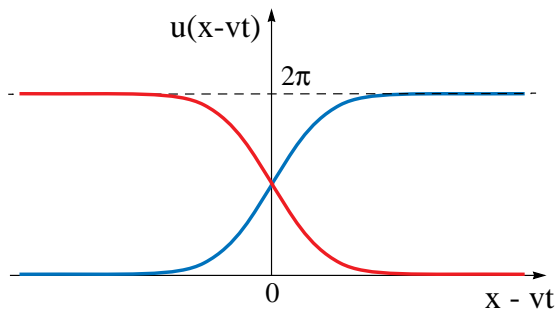
6

FIG. 8. A schematic plot of a kink-soliton and antikink-soliton solutions for the chain of pendulums shown in Fig. 7.

$n,t)$. A Tylor expansion of $\theta(n+1,t)$ and $\theta(n-1,t)$ around $\theta(n,t)$ turns the discrete sine-Gordon equation into the partial differential equation

$$\frac{\partial^2 \theta(x,t)}{\partial t^2} - c_0^2 \frac{\partial^2 \theta(x,t)}{\partial x^2} + \omega_0^2 \sin \theta = 0. \qquad (8)$$

The equation is called the *sine-Gordon* equation, and it has been extensively studied in soliton theory because it has exceptional mathematical properties. In particular, it has a soliton solution

$$u(x-vt) = 4 \arctan\left[\exp\left(\pm\frac{\omega_0}{c_0}\frac{x-vt}{\sqrt{1-v^2/c_0^2}}\right)\right], \quad (9)$$

which is plotted in Figs. 7 and 8. The ($\pm$) signs correspond to localized soliton solutions which travel with the opposite screw senses: they are respectively called a *kink* soliton and an *antikink* soliton. They are shown in Fig. 8: the pendulums rotate from 0 to 2π for the kink and from 0 to -2π for the antikink.

As the KdV equation, the sine-Gordon equation also contains dispersion and nonlinearity. However, in the sine-Gordon equation, both dispersion and nonlinearity appear in the same term $\omega_0^2 \sin \theta$, where ω_0 is a characteristic frequency of a system.

The topological nature of solitons in the chain of pendulums can be easily demonstrated by plotting the gravity potential acting on the pendulums versus θ and the position x of the pendulum. As one can see in Fig. 9, each kink joints two successive equilibrium states (potential minima). Thus, the kink-soliton can be considered as a *domain wall* between two degenerate energy minima. The topological soliton is an excitation which interpolates between these minima.

In the expression of the soliton solution, one can see that a topological soliton cannot travel faster than c_0 which represents the velocity of linear waves (in solids, the longitudinal sound velocity). As the soliton velocity v approaches c_0, the soliton remains constant but its width gets narrower owing to the Lorentz contraction of its profile, given by $d\sqrt{1-v^2/c_0^2}$, where $d = c_0/\omega_0$ is
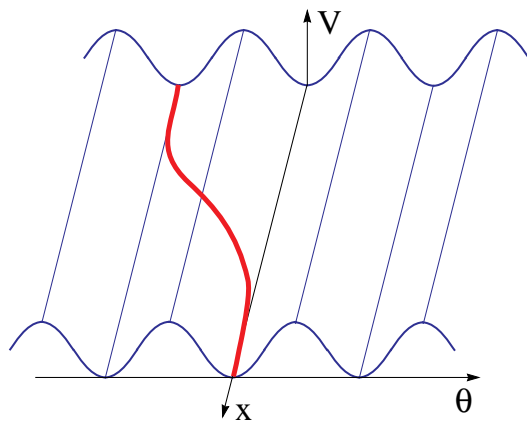

FIG. 9. Sketch of the sinusoidal potential of the pendulum chain. The solid curve shows the trajectory of the kink-soliton which can be considered as a domain wall between two degenerate energy minima.

a *discreteness* parameter. Thus, the topological solitons behave like relativistic particles.

From the condition $c_0^2/a^2 \gg \omega_0^2$ (see above), the discreteness parameter $d = c_0/\omega_0$ is much larger than the distance between pendulums, $d \gg a$. If $d \simeq a$, the angle of rotation varies abruptly from one pendulum to the next, and the continuum (long-wavelength) approximation cannot be used.

Comparing topological and nontopological solitons, it is worth remarking that the amplitude of the kink is independent of its velocity and, when the velocity $v = 0$, the soliton solution reduces to

$$u(x) = 4 \arctan[\exp(\pm x/d)]. \qquad (10)$$

Thus, by contrast to nontopological solitons, *the kink soliton may be entirely static*, losing its wave character. The second feature of topological solitons (kinks) is that they have antisolitons (antikinks) which are analogous to antiparticles. In contrast, for nontopological solitons, there are no antisolitons.

By using such a simple mechanical device shown in Fig. 7, it is easy to check experimentally the exceptional properties of the topological solitons. Launching a soliton and keeping on agitating the first pendulum, it is possible to test the ability of the soliton to propagate over a sea of linear waves. The particle-like properties appear clearly if one static soliton is created in the middle of the chain and then a second one is sent. The collision looks to the observer exactly similar to a shock between elastic marbles. Thus, the pendulum chain provides an experimental device which convincingly demonstrate the unique properties of the soliton.

In addition to the kink and antikink solutions, the sine-Gordon equation also has solutions in the form of oscillating pulses called a *breather* or *bion* (meaning a "living particle"). Breathers can be considered as a soliton-antisoliton bound state. An example of a breather is
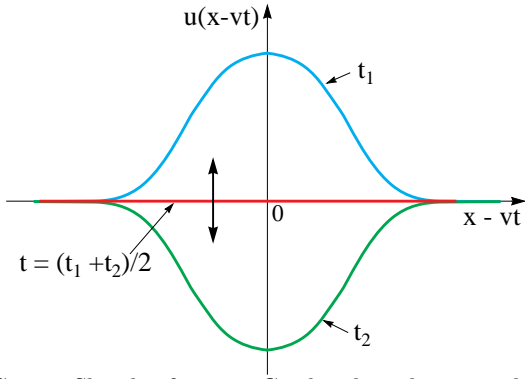
FIG. 10. Sketch of a sine-Gordon breather or a bion at different times t.

shown in Fig. 10. As other topological solitons, breathers can move with a constant velocity or be entirely static. Theoretically, breathers interact with other breathers and other solitons in the same manner as all topological solitons do. However, in reality, breather-type solitons can be easily destroyed by almost any type of perturbation.

Stationary breathers are pulsating objects. If, in the chain of pendulums shown in Fig. 7, one launches a kink and antikink (with the opposite screw sense) with sufficiently low velocity, one can observe a bounded pair that is a breather solution. Nevertheless, owing to dissipation effects present on the real line, only a few breathing oscillations can be observed. The oscillations then decrease with time and energy is radiated onto the line.

VIII. DIFFERENT CATEGORIES OF SOLITONS

There are a few ways to classify solitons. For example, as discussed above, there are *topological* and *nontopological* solitons. Independently of the topological nature of solitons, all solitons can be divided into two groups by taking into account their profiles: *permanent* and *time-dependent*. For example, kink solitons have a permanent profile (in ideal systems), while all breathers have an internal dynamics, even, if they are static. So, their shape oscillates in time. The third way to classify the solitons is in accordance with nonlinear equations which describe their evolution. Here we discuss common properties of solitons on the basis of the third classification, i.e. in accordance with nonlinear equations which describe the soliton solutions.

Up to now we have considered two nonlinear equations which are used to describe soliton solutions: the KdV equation and the sine-Gordon equation. There is the third equation which exhibits true solitons—it is called the *nonlinear Schrödinger* (NLS) equation. We now summarize soliton properties on the basis of these three equations, namely, the Korteweg-de Vries equation:

$$u_t = 6uu_x - u_{xxx};$$ (11)

the sine-Gordon equation:

$$u_{tt} = u_{xx} - \sin u,$$ (12)

and the nonlinear Schrödinger equation:

$$iu_t = -u_{xx} \pm |u|^2 u,$$ (13)

where u_z means $\frac{\partial u}{\partial z}$. For simplicity, the equations are written for the dimensionless function u depending on the dimensionless time and space variables.

There are *many* other nonlinear equations (i.e. the Boussinesq equation) which can be used for evaluating solitary waves, however, these three equations are particularly important for physical applications. They exhibit the most famous solitons: the KdV (pulse) solitons, the sine-Gordon (topological) solitons and the *envelope* (or NLS) solitons. All the solitons are one-dimensional (or quasi-one-dimensional). Figure 11 schematically shows these three types of solitons. Let us summarize common features and individual differences of the three most important solitons.

A. The KdV solitons

The exact solution of the KdV equation is given by Eq. (2). The basic properties of the KdV soliton, shown in Fig. 11a, can be summarized as follows [7]:

  i. Its amplitude increases with its velocity (and vice versa). Thus, they cannot exist at rest.

  ii. Its width is inversely proportional to the square root of its velocity.

  iii. It is a unidirectional wave pulse, i.e. its velocity cannot be negative for solutions of the KdV equation.

  iv. The sign of the soliton solution depends on the sign of the nonlinear coefficient in the KdV equation.

The conservation laws for the KdV solitons represent the conservation of mass

$$M = \frac{1}{2} \int u\,dx;$$ (14)

momentum

$$P = -\frac{1}{2} \int u^2\,dx;$$ (15)

energy

$$E = \frac{1}{2} \int (2u^2 + u_x^2)\,dx,$$ (16)

(a)
KdV equation

(b)
sine-Gordon
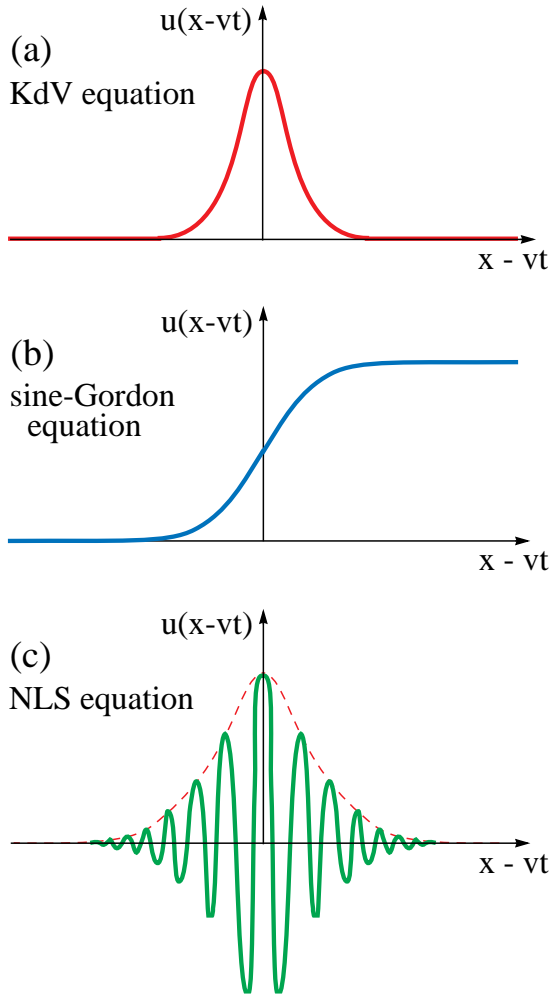equation

(c)
NLS equation

FIG. 11. Schematic plots of the soliton solutions of: (a) the Korteweg–de Vries equation; (b) the sine-Gordon equation, and (c) the nonlinear Schrödinger equation.

and center of mass

$$Mx_s(t) = \frac{1}{6} \int xu \, dx = tP + const. \qquad (17)$$

The KdV solitons are nontopological, and they exist in physical systems with weakly nonlinear and with weakly dispersive waves. When a wave impulse breaks up into several KdV solitons, they all move in the same direction (see, for example, Fig. 2). The collision of two KdV solitons is schematically shown in Fig. 3. Under certain conditions, the KdV solitons may be regarded as particles, obeying the standard laws of Newton's mechanics. In the presence of dissipative effects (friction), the KdV solitons gradually decelerate and become smaller and longer, thus, they are "mortal."

B. The topological solitons

The exact solution of the sine-Gordon equation is given by Eq. (9). The basic properties of a topological (kink) soliton shown in Fig. 11b can be summarized as follows [7]:

  i. Its amplitude is independent of its velocity—it is constant and remains the same for zero velocity, thus the kink may be static.

 ii. Its width gets narrower as its velocity increases, owing to Lorentz contraction.

iii. It has the properties of a relativistic particle.

 iv. The topological kink which has a different screw sense is called an *antikink*.

For the chain of pendulums shown in Fig. 7, the energy of the topological (kink) soliton, E_K, is determined by

$$E_K = \frac{m_0 c_0^2}{\sqrt{1 - \frac{v^2}{c_0^2}}}, \qquad (18)$$

where c_0 is the velocity of *linear* waves, and the soliton mass m_0 is given by

$$m_0 = 8\frac{I}{a}\frac{\omega_0}{c_0} = 8\frac{I}{a}\frac{1}{d}. \qquad (19)$$

One can also introduce the relativistic momentum

$$p_K = \frac{m_0 v}{\sqrt{1 - \frac{v^2}{c_0^2}}}. \qquad (20)$$

At rest ($v = 0$) one has $p = 0$, and the static soliton energy is

$$E_{0,K} = m_0 c_0^2. \qquad (21)$$

Topological solitons are extremely stable. Under the influence of friction, these solitons only slow down and eventually stop and, at rest, they can live "eternally." In an infinite system, the topological soliton can only be destroyed by moving a semi-infinite segment of the system above a potential maximum. This would require an infinite energy. However, the topological soliton can be annihilated in a collision between a soliton and an anti-soliton. In an integrable system having exact soliton solutions, solitons and anti-solitons simply pass through each other with a phase shift, as all solitons do, but in a real system like the pendulum chain which has some dissipation of energy, the soliton-antisoliton equation may destroy the nonlinear excitations. Figure 12 schematically shows a collision of a kink and an antikink in an integrable system which has soliton solutions. In integrable
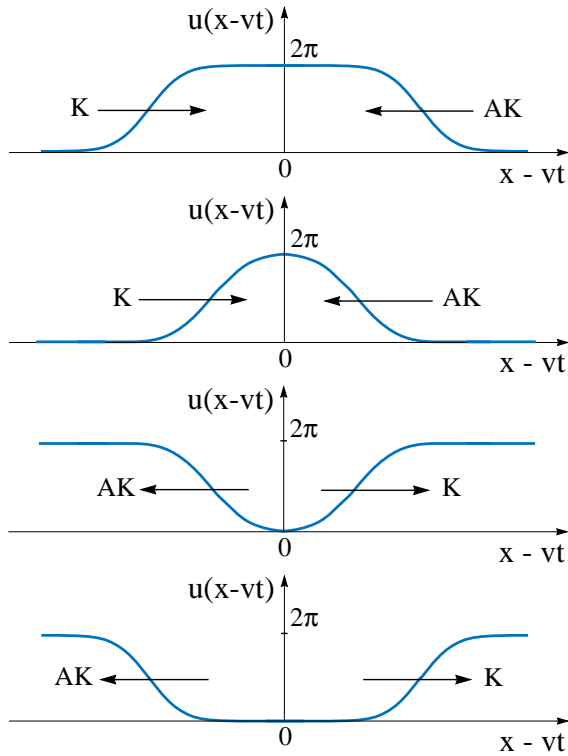
FIG. 12. Sketch of a collision between a kink (K) and an antikink (AK). The phase shift after the collision is not indicated.

systems, the soliton-breather and breather-breather collisions are similar to the kink-antikink collision shown in Fig. 12.

The sine-Gordon equation has almost become ubiquitous in the theory of condensed matter, since it is the simplest nonlinear wave equation in a periodic medium.

C. The envelope solitons

The NLS equation is called the *nonlinear* Schrödinger equation because it is formally similar to the Schrödinger equation of quantum mechanics

$$\left[i\hbar\frac{\partial}{\partial t} + \frac{\hbar^2}{2m}\frac{\partial^2}{\partial x^2} - U\right]\Psi(x,t) = 0, \qquad (22)$$

where U is the potential, and $\Psi(x,t)$ is the wave function.

The NLS equation describes self-focusing phenomena in nonlinear optics, one-dimensional self-modulation of monochromatic waves, in nonlinear plasma etc. In the NLS equation, the potential U is replaced by $|u|^2$ which brings into the system self-interaction. The second term of the NLS equation is responsible for the dispersion, and the third one for the nonlinearity. A solution of the NLS equation is schematically shown in Fig. 11c. The shape of the enveloping curve (the dashed line in Fig. 11c) is given by

$$u(x,t) = u_0 \times sech((x-vt)/\ell), \qquad (23)$$

where 2ℓ determines the width of the soliton. Its amplitude u_0 depends on ℓ, but the velocity v is *independent* of the amplitude, distinct from the KdV soliton. The shapes of the envelope and KdV solitons are also different: the KdV soliton has a $sech^2$ shape. Thus, the envelope soliton has a slightly wider shape. However, other properties of the envelope solitons are similar to the KdV solitons, thus, they are "mortal" and can be regarded as particles. The interaction between two envelope solitons is similar to the interactions between two KdV solitons (or two topological solitons), as shown in Fig. 3.

In the envelope soliton, the stable groups have normally from 14 to 20 humps under the envelope, the central one being the highest one. The groups with more humps are unstable and break up into smaller ones. The waves inside the envelope move with a velocity that differs from the velocity of the soliton, thus, the envelope soliton has an *internal* dynamics. The relative motion of the envelope and carrier wave is responsible for the internal dynamics of the NLS soliton.

The NLS equation is inseparable part of nonlinear optics where the envelope solitons are usually called *dark* and *bright* solitons, and became quasi-three-dimensional. We shall briefly discuss the optical solitons below.

D. Solitons in real systems

As a final note to the presentation of the three types of solitons, it is necessary to remark that real systems do not carry exact soliton solutions in the strict mathematical sense (which implies an infinite life-time and an infinity of conservation laws) but *quasi*-solitons which have most of the features of true solitons. In particular, although they do not have an infinite life-time, quasi-solitons are generally so long-lived that their effect on the properties of the system are almost the same as those of true solitons. This is why physicists often use the word soliton in a relaxed way which does not agree with mathematical rigor.

In the following sections, we consider a few examples of solitons in real systems, which are useful for the understanding of the mechanism of high-T_c superconductivity.

IX. SOLITONS IN THE SUPERCONDUCTING STATE

Solitons are literally everywhere. The superconducting state is not an exception: vortices and *fluxons* are topological solitons. Fluxons are quanta of magnetic flux, which can be studied in *long Josephson junctions.* A long Josephson junction is analogous to the chain of atoms studied by Frenkel and Kontorova. The sine-Gordon
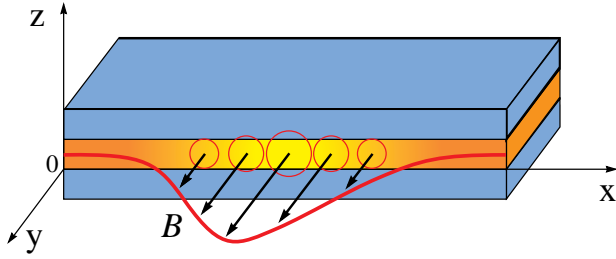
FIG. 13. Sketch of a soliton in a long Josephson junction.

equation provides an accurate description of vortices and fluxons.

In a type-II superconductor, if the magnitude of an applied magnetic field is larger than the lower critical field, B_{c1}, the magnetic field begins to penetrates the superconductor in microscopic vortices which form a regular lattice. Vortices in a superconductor are similar to vortices in the ideal liquid, but there is a dramatic difference—they are *quantized*. Inside the vortex tube, there exists a magnetic field. The magnetic flux supported by the vortex is a multiple of the *quantum magnetic flux* $\Phi_0 \equiv hc/2e$, where c is the speed of light; h is the Planck constant, and e is the electron charge. The vortices in type-II superconductors are a pure and beautiful physical realization of the sine-Gordon (topological) solitons. Their extreme stability can be easily understood in terms of the Ginzburg-Landau theory of superconductivity which contains a system of nonlinear coupled differential equations for the vector potential and the wave function of the superconducting condensate. Thus, topological solitons in the form of vortices were found in the superconducting state 20 years earlier than the superconducting state itself was understood.

Let us now consider fluxons in a long Josephson junction. An example of a *long* superconductor-insulator-superconductor (SIS) Josephson junction is schematically shown in Fig. 13. The insulator in the junction is thin enough, say 10–20 Å, to ensure the overlap of the wave functions. Due to the Meissner effect, the magnetic field may exist only in the insulating layer and in adjacent thin layers of the superconductor.

As discussed in Chapter 2 in [14], the magnitude of the zero-voltage current resulting from the tunneling of Cooper pairs, known as the *dc* Josephson effect, depends on the phase difference between two superconductors as

$$I = I_c \sin \varphi, \qquad (24)$$

where $\varphi = \varphi_2 - \varphi_1$ is the phase difference, and I_c is the critical Josephson current.

The oscillating current of Cooper pairs that flows when a steady voltage V is maintained across a tunnel barrier is known as the *ac* Josephson effect. The phase difference between the two superconductors in the junction is given by

$$\frac{d\varphi}{dt} = \frac{2e}{\hbar} V. \qquad (25)$$

Taking into account the inductance and the capacitance of the junction, one can easily get a sine-Gordon equation for $\varphi(x,t)$ forced by a right-hand side term which is associated with the applied bias. For a long Josephson junction, the nonlinear equation exactly coincides with Eq. (8). In the long Josephson junction, the sine-Gordon solitons describe quanta of magnetic flux, expelled from the superconductors, that travels back and forth along the junction. Their presence, and the validity of the soliton description, can be easily checked by the microwave emission which is associated with their reflection at the ends of the junction.

For the Josephson junction, the ratio $\lambda_J = c_0/\omega_0$ [see Eq. (8)] gives a measure of the typical distance over which the phase (or magnetic flux) changes, and is called the *Josephson penetration length*. This quantity allows one to define precisely a *small* and a *long* junction. A junction is said to be long if its geometric dimensions are large compared with λ_J. Otherwise, the junction is small. The Josephson length is usually much larger than the London penetration depth λ_L.

The moving fluxon has a kink shape, which is accompanied by a *negative* voltage pulse and a *negative* current pulse, corresponding to the space and time derivatives of the fluxon solution. In Fig. 13, the arrows in the y direction represent the magnetic field, and the circles show the Josephson currents producing the magnetic field.

A very useful feature of the Josephson solitons is that they are not difficult to operate by applying bias and current to the junction. By using artificially prepared inhomogeneities one can make bound state of solitons. In this way one can store, transform and transmit information. In other words, long Josephson junctions can be used in computers. One of the most useful properties of such devices would be very high performance speed. Indeed, the characteristic time may be as small as 10^{-10} sec, while the size of the soliton may be less than 0.1 mm. The main problem for using the Josephson junctions in electronic devices is the cost of cooling refrigerators. However, I am absolutely sure that they will be commercially used in electronics if room-temperature superconductors become available.

X. TOPOLOGICAL SOLITONS IN POLYACETYLENE

Let us consider topological solitons and *polarons* in solids. One-dimensional polarons are breathers, consequently, they can be considered as a soliton-antisoliton (kink-antikink) bound state. The term "polaron" should not be confused with the Holtstein (small) polaron which is three-dimensional, and represents a self-trapped state in solids (see Section XII).
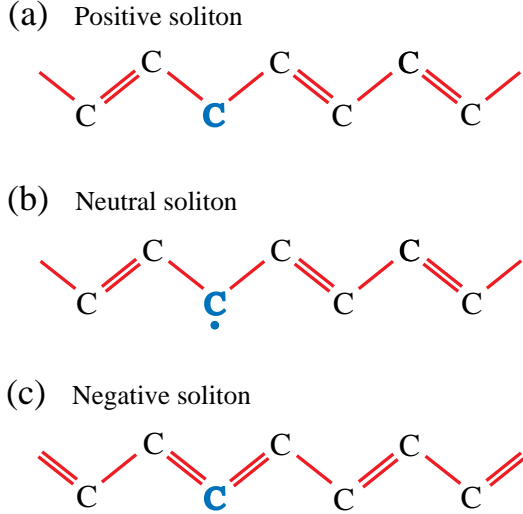
11

FIG. 14. Formula of polyacetylene showing the possibility to have a topological soliton: (a) positive; (b) neutral, and (c) negative.
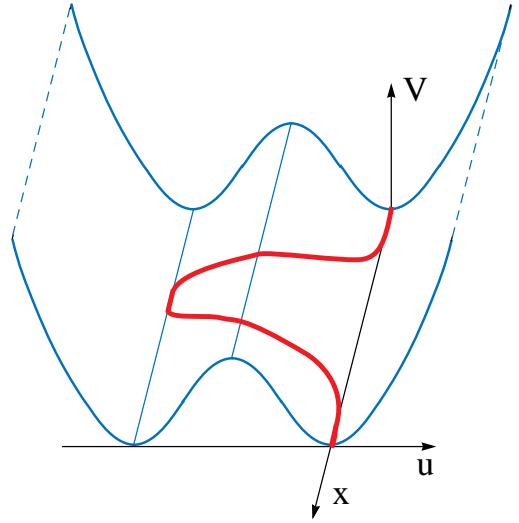

FIG. 15. Sketch of the double-well potential for *trans*-polyacetylene. The solid curve shows the trajectory of the kink-antikink (breather) solution.

Polyacetylene, $(CH)_x$, is the simplest linear conjugated polymer. Polyacetylene exists in two isomerizations: *trans* and *cis*. Let us consider the *trans*-polyacetylene. The structure of *trans*-polyacetylene is schematically shown in Fig. 14. The important property of *trans*-polyacetylene is the double degeneracy of its ground state: the energy for the two possible patterns of alternating short (double) and long (single) bonds. The double-well potential is schematically shown in Fig. 15. In double-well potential, a kink cannot be followed by another kink like, for example, in a potential with infinite number of equilibrium states, shown in Fig. 9: a kink can be followed only by an antikink, which connect the two potential wells, as shown in Fig. 15. In *cis*-polyacetylene, the two ground-state configurations have different energies. Therefore, in *cis*-polyacetylene, the two-well potential is asymmetrical. Further we consider only the *trans*-polyacetylene configuration, sometimes, dropping the prefix "trans".

Undoped polyacetylene which has a half-filled band is an insulator with a charge gap of 1.5 eV. The gap is partially attributed to the so-called Peierls instability of the one-dimensional electron gas. Upon doping, polyacetylene becomes highly conducting. The significant overlap between the orbitals of the neighboring carbon atoms results in a relatively broad band (called π-band) with a width of 10 eV. The polyacetylene chains are only weakly coupled to each other: the distance between the nearest carbon atoms belonging to different chains is about 4.2 Å, which is three times larger than the distance between the nearest carbon atoms in the chains. As a consequence, the interchain hopping amplitude is about 30 times smaller than the hopping amplitude along the chain, which makes the intrinsic properties of polyacetylene quasi-one-dimensional.

As a consequence of the two degenerate ground state in *trans*-polyacetylene, it is natural to expect the existence of excitations in polyacetylene in the form of topological solitons, or moving domain walls, separating the two degenerate minima. Depending on doping, there exist 3 different types of topological solitons (kinks) in polyacetylene, having different quantum numbers. As shown in Fig. 14a, the removal of one electron from a polyacetylene chain creates a positively charged soliton with charge of $+e$ and spin zero [8]. The addition of one electron to a polyacetylene chain generates a neutral soliton with spin of $1/2$, as shown in Fig. 14b. Figure 14c shows the case when two electrons are added to a polyacetylene chain. In this case, the soliton is negatively charged, having spin zero. Since these three kinds of solitons differ only by the occupation number of the zero energy state, the all have the same creation energy given by

$$E_s = \frac{2}{\pi}\Delta, \tag{26}$$

where 2Δ is the width of the charge gap which separates the valence band and the conduction band. All three solitons occupy the midgap state of the charge gap, as schematically shown in Fig. 16b. Thus, to create a soliton is more energetically profitable than to add one electron to the conduction band, $E_s < 2\Delta$. Figure 16a shows a *tanh*-shaped kink which connects the two electron bands and the electron density of states of the midgap state shown in Fig. 16b (compare with Fig. 6). In Fig. 16a, the spatial density of states is determined by $|\psi(x)|^2$, where

$$\psi(x) = \frac{C}{\cosh(x/d)} = C \times sech(x/d), \tag{27}$$
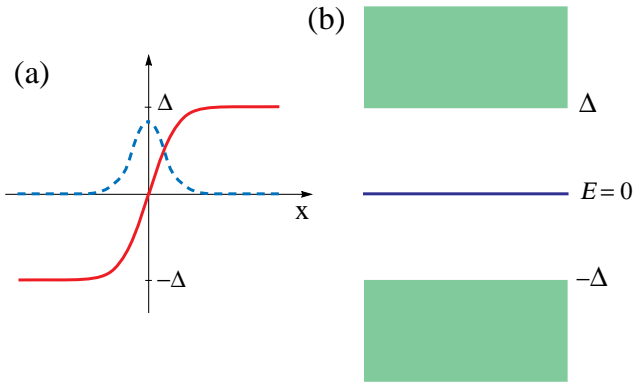
and C and d are constants.

FIG. 16. (a) A schematic plot of a topological soliton (thick curve) in *trans*-polyacetylene and the electron density of states $|\psi(x)|^2$ for the intragap state (dashed curve). The vertical axis for the density of states is not shown. (b) The spectrum of electron states for the soliton lattice configuration. The lower band corresponds to the valence band, and the upper band to the conduction band.
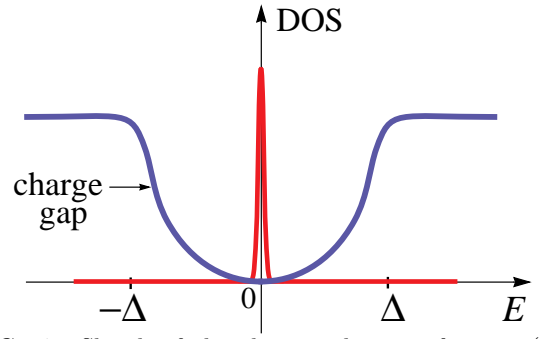

FIG. 17. Sketch of the electron density of states (DOS) per unit energy interval in *trans*-polyacetylene for the soliton lattice configuration. The height of the soliton peak depends on the density of added or removed electrons [9].

In Fig. 16a, the density of states is presented as a function of soliton position along the main polyacetylene axis. Figure 17 depicts the density of states in doped polyacetylene as a function of energy having the origin at the middle of the charge gap. The density of states shown in Fig. 17 corresponds to the total number of energy levels per unit volume which are available for possible occupation by electrons. Since the peak in the spatial density of states, shown in Fig. 16a, is not the delta function, but has a finite width, then, according to the Fourier transform, the width of corresponding peak in the spectral density of states is also finite. So, the width of the soliton peak shown schematically in Fig. 17 is finite. In Fig. 17, the height of the soliton peak depends on the density of added or removed electrons: the height increases as the electron density increases [9]. However, one should realize that there exists a maximum density of added or removed electrons, above which the charge gap collapses, and polyacetylene becomes metallic.

The model was created in order to explain a very unusual behavior of the spin susceptibility in *trans*-polyacetylene. Upon doping, pristine polyacetylene becomes highly conducting. Strangely, the spin susceptibility of *trans*-polyacetylene remains small well into the conducting regime. Using the model, this strange behavior can be well understood: upon doping, the charge carriers in polyacetylene are not conventional electrons and holes, but spinless solitons (kinks).

Following the original analysis [8], the model has been refined and it has been shown that the most probable defects are not the topological solitons but breathers (or polarons) which can be considered as a soliton-antisoliton bound state. In double-well potential, a kink can only be followed by an anti-kink, as shown in Fig. 15. Thus, the breather (polaron) solution is a sum of two *tanh* functions:

$$\Delta_{pol} = \Delta - v_F K \left[\tanh\left(K\left(x + \frac{R}{2}\right)\right) - \tanh\left(K\left(x - \frac{R}{2}\right)\right)\right],$$
(28)

where R is the distance between the soliton and antisoliton; v_F is the velocity on the Fermi surface, and K is determined by

$$v_F K = \Delta \tanh(KR).$$
(29)

The spectrum of electron states for Δ_{pol} consists of a valence band (with the highest energy $-\Delta$), a conduction band (with the lowest energy $+\Delta$), and two localized intragap states with energies $\pm E_0(R)$, as shown in Fig. 18b, where

$$E_0(R) = \frac{\Delta}{\cosh(KR)}.$$
(30)

The two intragap states are symmetric and antisymmetric superposition of the midgap state localized near the kink and antikink:

$$\psi_{\pm}(x) = \frac{1}{2}\left(\frac{\sqrt{K/2}}{\cosh(K(x - R/2))}|-\rangle \pm \frac{\sqrt{K/2}}{\cosh(K(x + R/2))}|+\rangle \right).$$
(31)

These results for the electron wave function hold for any distance R between the kink and antikink. However, the configuration Eq. (28) is only self-consistent if

$$R_{sc} = \sqrt{2}\ln(1 + \sqrt{2})\xi_0,$$
(32)

where $\xi_0 = v_F/\Delta$ denotes a correlation length. Then, $K\xi_0 = 1/\sqrt{2}$ and $E_0(R_c) = \Delta/\sqrt{2}$.

The occupation of the two intragap states $\psi_{\pm}$ cannot be arbitrary: the solution is self-consistent if there is either one electron in the negative energy state ψ_- and no electrons in the positive energy state ψ_+, or if ψ_- is doubly occupied and ψ_+ is occupied by one electron. Only charged polarons are stable, thus they have charge $\pm e$
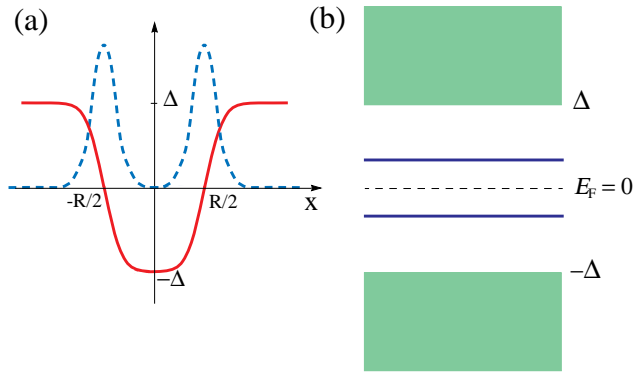
13

FIG. 18. A schematic plot of a soliton-antisoliton lattice configuration (thick curve) in *trans*-polyacetylene and the electron density of states $|\psi(x)|^2$ for the two intragap state (dashed curve). The vertical axis for the density of states is not shown. (b) The spectrum of electron states for the soliton-antisoliton lattice configuration. The lower band corresponds to the valence band, and the upper band to the conduction band.

and spin 1/2. The polaron has the quantum numbers of an electron (a hole). In other words, the polaron is a bound state of a charged spinless soliton and a neutral soliton with spin 1/2. Figure 18a shows a bound state of a kink and an antikink separated by distance R, and the electron density of states of the two intragap states shown in Fig. 18b.

By contrast, a charged kink and a charged antikink do not form a bound state, as they repel each other, even, in the absence of the Coulomb interaction. For a given density of added or removed electrons, this repulsion forces the charged kinks and antikinks to form a periodic lattice. At small density of added charges, the soliton lattice has a lower energy than the polaron lattice, since the kink creation energy E_s [see Eq. (26)] is smaller than the energy of polaron creation, which is given by

$$E_p = \frac{2\sqrt{2}}{\pi}\Delta = \sqrt{2}E_s. \tag{33}$$

In Fig. 18a, the density of states is presented as a function of soliton and antisoliton positions along the main polyacetylene axis. Figure 19 *schematically* depicts the density of states in doped polyacetylene as a function of energy having the origin at the middle of the charge gap. Since the occupation of the two intragap states cannot be arbitrary, the heights of the two peaks shown in Fig. 19 are, in fact, different: the right-hand peak should be lower than the left-hand peak.

Finally, it is worth emphasizing two aspects of kink-antikink bound state in any nonlinear system. First, the *distance* between the two peaks in the spectral density of states, shown in Figs. 18b and 19, depends on the *real distance* between the kink and the antikink, as schematically depicted in Fig. 18a. Second, the spatial *and* spectral densities of states of any kink-(anti)kink bound state
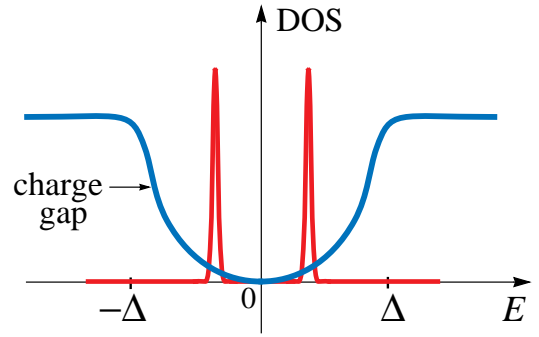

FIG. 19. Sketch of the electron density of states (DOS) per unit energy interval in *trans*-polyacetylene for the soliton-antisoliton lattice configuration. The height of the soliton-antisoliton peaks depends on the density of added or removed electrons [9].

(if such exists) are not sensitive to the "polarity" of the two kinks: the density of states of a bound state of two (anti)kinks (for example, in the periodic potential shown in Fig. 9) coincides with the density of states of a kink-antikink bound state: compare the dashed curves in Figs. 20 and 18a.
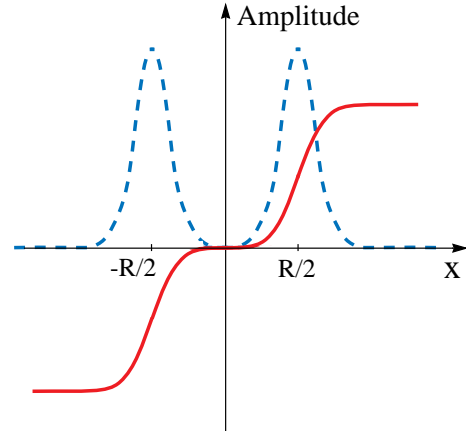

FIG. 20. A schematic plot of two kinks (solid curve), for example, in infinite-well potential shown in Fig. 9, and the corresponding density of states (dashed curve). Compare with Fig. 18a.

XI. MAGNETIC SOLITONS

Solitons are not restricted to the macroscopic world—they exist on the microscopic scale too.

Historically, in the theory of solid state magnetism, nonlinearities were considered small and were described in terms of linear theory. In the linear approximation, eigen-excitations in the magnetic medium were considered as an ideal gas of non-interacting spin waves or *magnons*. Taking into account that nonlinearities in real medium always present, the solution of nonlinear equation of motion for magnetic excitations represents a mag-

netic soliton. The term "magnetic soliton" has a broad meaning: there exist magnetic kinks and envelope solitons which are described by the sine-Gordon and NLS equations, respectively.

Magnetic *kink* solitons clearly show up in the properties of quasi-one-dimensional magnetic materials in which spins interact strongly along one axis of the crystal and very weakly along the other axes. Such spin chains are qualitatively similar to the pendulum chain shown in Fig. 7. Let us assume that the pendulums in Fig. 7 represents spins in a spin chain. Such a situation when all spins in the chain are oriented in the same direction (down in Fig. 7) corresponds to a *ferromagnetic* ordering. And a torsion of the spin lattice, shown in Fig. 7, can propagate as a soliton in the crystal. An *antiferromagnetic* ordering represents a staggered spin orientation in the chain, i.e. for each spin in the chain, its nearest neighbors have the opposite orientation. In antiferromagnetically ordered materials, a torsion of the spin lattice also corresponds to a magnetic kink-soliton. Magnetic kink-solitons are domain walls which can be moving or stationary, and described by the sine-Gordon equation. These solitons are usually created thermally and their dynamics can be studied very accurately by using neutron scattering. The soliton concept is again precious because the solitons can be treated as quasiparticles and the results can be obtained by investigating a "soliton gas."

For a qualitative understanding of magnetic solitons, we need not look into details of so-called *exchange* forces between spins. As distinct from quantum exchange forces that really act among the nearest neighbors, these exchange forces are classical and have a *long range*. Accordingly, it becomes energetically favorable for ferromagnetically ordered spins to divide into many groups. In one half of these groups, the spins look up, in the other half, they look down. These groups are also called *domains*, and the borders between domains—domain walls which are similar to the Frenkel-Kontorova dislocations. Therefore, they are solitons, and their evolution is described by the sine-Gordon equation. Like dislocations, the domain walls may move along the crystal if there is no obstruction from the crystal imperfections or from other domain walls.

The latter domain walls are somewhat easier to observe than the dislocations. A typical distance between two magnetic domain walls is about 1 mm, and their thickness is typically 10 μm or so. Covering well-polished surface of a ferromagnetic sample with a thin powder of a magnetic material, it turns out that its particles gather near the domain walls. Thus, *the particles are attracted by the domain walls.*

As mentioned above, there also exist magnetic *envelope* solitons. In the linear approximation, a propagating linear packet of spin waves is spread by dispersion because individual spin waves in the packet are totally independent of each other. The solution of equation of
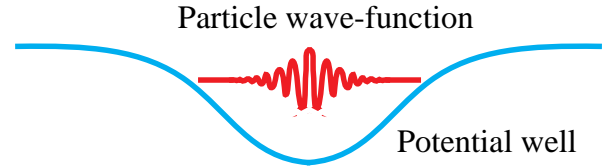

Particle wave-function

Potential well

FIG. 21. Sketch of a self-trapped state: a particle (electron or hole) with a given wave function deforms the lattice inducting a potential well which in turn traps the particle.

motion for the magnetization, which contains nonlinear effects, represents a magnetic envelope soliton. The latter is a cluster or a bound state of large number of spin waves where the attraction between spin waves compensate the spreading effect of dispersion. The existence of spin wave envelope solitons was predicted theoretically, and later they were experimentally observed in the microwave frequency range. This type of magnetic solitons are described by the NLS equation.

XII. SELF-TRAPPED STATES: THE DAVYDOV SOLITON

Solitons represent localized states and, in real systems, there exist *self-localized* states. In other words, there are cases when, in exchange of interaction with a medium, an excitation or a particle locally deforms the medium in a way that it is attracted by the deformation. In the context of condensed matter physics, Landau proposed that an electron in a solid can be considered as being "dressed" by its self-created polarization field, forming a quasiparticle. When the particle-field interaction (electron-phonon coupling) is strong, both the particle wave function and lattice deformation are localized. In the three-dimensional case, this localized entity is known as a (Holstein) polaron and, in one dimension a Davydov soliton or *electrosoliton*. Their integrity is maintained owing to the dynamical balance between the dispersion (exchange inter-site interaction) and the nonlinearity (phonon-electron coupling). Figure 21 schematically shows a self-trapped state of a particle (a small polaron or a Davydov soliton). In a self-trapped state, *both* the particle-wave function and lattice deformation are *localized*.

Before we discuss the Davydov bisoliton model of high-T_c superconductivity, we consider first the concept of the Davydov soliton [10, 11].

To describe the self-focusing phenomena, the NLS equation is used,

$$\left[i\hbar \frac{\partial}{\partial t} + \frac{\hbar^2}{2m} \frac{\partial^2}{\partial x^2} + G|\psi(x,t)|^2 \right] \psi(x,t) = 0. \quad (34)$$

The equation is written in the long-wave approximation when the excitation wavelength λ is much larger than the

characteristic dimension of discreteness in the system, i.e. under the condition $ka = 2\pi a/\lambda \ll 1$. The equation describes the complex field $\psi(x,t)$ with self-interaction. The function $|\psi|^2$ determines the position of a quasiparticle of mass m. The second term in the NLS equation is responsible for the dispersion, and the third one for nonlinearity. The coefficient G characterizes the intensity of the nonlinearity.

When the nonlinearity is absent $(G = 0)$, the NLS equation has solutions in the form of plane waves,

$$\psi(x,t) = \Phi_0 \exp[i(ka - \omega(k)t)], \qquad (35)$$

with the square dispersion law $\omega(k) = \hbar k^2/2m$. With nonlinearity $(G \neq 0)$ in the system having a translational invariance, the excited states move with constant velocity V. Therefore it is convenient to study solutions of the NLS equation in the reference frame

$$\zeta = (x - Vt)/a, \qquad (36)$$

moving with constant velocity. In this reference frame the NLS equation has solutions in the form of a complex function

$$\psi(x,t) = \Phi(\zeta) \exp[i(kx - \omega t)], \ k = mV/\hbar, \qquad (37)$$

where the real function $\Phi(\zeta)$ satisfies the nonlinear equation

$$\left[\hbar\omega - \frac{1}{2}mV^2 + J\frac{\partial^2}{\partial x^2} + G_0\Phi^2(\zeta) \right] \Phi(\zeta) = 0, \qquad (38)$$

where $J = \hbar^2/2ma^2$.

The last equation has two types of solutions: nonlocalized and localized ones. The nonlocalized solution corresponds to a constant value of the amplitude $\Phi(\zeta) = \Phi_0$ and the dispersion law

$$\hbar\omega = \frac{1}{2}mV^2 - G_0\Phi_0^2. \qquad (39)$$

If a particle is at a distance L, then $\Phi_0^2 = L^{-1}$ and, in the limit $L \to \infty$, the second term in the last equation tends to zero.

The localized solution of the NLS equation normalized by the condition

$$\int \Phi^2(\zeta)d\zeta = 1, \qquad (40)$$

is represented, as we already know, by the bell-shaped function

$$\Phi(\zeta) = \sqrt{\frac{g}{2}} \times sech(g\zeta), \qquad (41)$$

with the dimensionless nonlinearity parameter g given by

$$g = G_0/4J. \qquad (42)$$

The function $\Phi(\zeta)$ is nonzero on a segment $\Delta\zeta \approx 2\pi/g$. The larger the nonlinearity parameter the smaller is the localization region.

The energy of localized excitations is determined by the expression

$$\hbar\omega = \frac{1}{2}mV^2 - Jg^2. \qquad (43)$$

In the localized solution found above, the nonlinearity is generated by the "self-action" of the field. Let us now study a self-trapping effect when two linear system interact with each other. As an example, we consider the excess electron in a quasi-one-dimensional atomic (molecular) chain. If neutral atoms (molecules) are rigidly fixed in periodically arranged sites na of a one-dimensional chain, then, due to the translational invariance of the system, the lowest energy states of an excess electron are determined by the conduction band. The latter is caused by the electron collectivization. In the continuum approximation, the influence of a periodic potential is taken into account by replacing the electron mass m_e by the effective mass $m = \hbar/2a^2J$ which is inversely proportional to the exchange interaction energy that characterizes the electron jump from one node site into another. In this approximation, the electron motion along an ideal chain corresponds to the free motion of a quasiparticle with effective mass m and electron charge.

Taking into account of small displacements of molecules of mass M $(\gg m)$ from their periodic equilibrium positions, there arises the short-range deformation interaction of quasiparticles with these displacements. When the deformation interaction is rather strong, the quasiparticle is self-localized. Local displacement caused by a quasiparticle is manifest as a potential well that contains the particle, as schematically shown in Fig. 21. In turn, the quasiparticle deepens the well.

A self-trapped state can be described by two coupled differential equations for the field $\psi(x,t)$ that determines the position of a quasiparticle, and the field $\rho(x,t)$ that characterizes local deformation of the chain and determines the decrease in the relative distance $a \to a - \rho(x,t)$ between molecules of the chain,

$$\left[i\hbar\frac{\partial}{\partial t} + \frac{\hbar^2}{2m}\frac{\partial^2}{\partial x^2} + \sigma\rho(x,t) \right] \psi(x,t) = 0, \qquad (44)$$

$$\left(\frac{\partial^2}{\partial t^2} - c_0^2\frac{\partial^2}{\partial x^2} \right) \rho(x,t) - \frac{a^2\sigma}{M}\frac{\partial^2}{\partial x^2}|\psi(x,t)|^2 = 0. \quad (45)$$

The first equation characterizes the motion of a quasiparticle in the local deformation potential $U = -\sigma\rho(x,t)$. The second equation determines the field of the local deformation caused by a quasiparticle. The system of the two equations are connected through the parameter σ of the interaction between a quasiparticle and local deformation. The quantity $c_0 = a\sqrt{k/M}$ is the longitudinal

sound velocity in the chain with elasticity coefficient k. When there is one quasiparticle in the chain, the function $\psi(x,t)$ is normalized by

$$\frac{1}{a}\int_{-\infty}^{\infty}|\psi(x,t)|^2 dx = 1. \qquad (46)$$

In the reference frame $\zeta = (x - Vt)/a$ moving with constant velocity V, the following equality $\partial\rho(x,t)/\partial t = -V/a \times \partial\rho/\partial\zeta$ holds. Then, the solution for $\rho(x,t)$ has the form

$$\rho(x,t) = \frac{\sigma}{k(1-s^2)}|\psi(x,t)|^2, \ \ s^2 = V^2/c_0^2 \ll 1. \qquad (47)$$

Substituting the values $\rho(x,t)$ into Eq. (44), we transform it to a nonlinear equation for the function $\psi(x,t)$,

$$\left[i\hbar\frac{\partial}{\partial t} + \frac{\hbar^2}{2m}\frac{\partial^2}{\partial x^2} + 2gJ|\psi(x,t)|^2\right]\psi(x,t) = 0. \qquad (48)$$

where

$$g \equiv \frac{\sigma^2}{2k(1-s^2)J} \qquad (49)$$

is the dimensional parameter of the interaction of a quasiparticle with a local deformation. Substituting the function

$$\psi(x,t) = \Phi(\zeta)\exp[i(kx - \omega t)], \ \ k = mV/\hbar \qquad (50)$$

into the Eq. (48) we get the equation

$$[\hbar\omega - \frac{1}{2}mV^2 - J\frac{\partial^2}{\partial\zeta^2} + 2gJ\Phi^2(\zeta)]\Phi(\zeta) = 0, \qquad (51)$$

for the amplitude function $\Phi(\zeta)$ normalized by $\int\Phi^2(\zeta)d\zeta = 1$. The solution of this equation is

$$\Phi(\zeta) = \frac{1}{2}\sqrt{g} \times sech(g\zeta/2), \qquad (52)$$

with the value

$$\hbar\omega = \frac{1}{2}mV^2 - D(s). \qquad (53)$$

The quantity

$$D(s) = \frac{1}{8}g^2 J \qquad (54)$$

determines the binding energy of a particle and the chain deformation produced by the particle itself. According to Eq. (52), a quasiparticle is localized in moving reference frame

$$\Delta\zeta = 2\pi/g, \qquad (55)$$

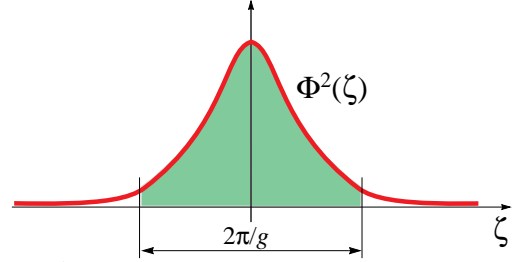as shown in Fig. 22. In this region, the field localization is characterized by the function

FIG. 22. A schematic plot of a self-trapped soliton. The soliton is very localized, having a size of $2\pi/g$.

$$\rho(\zeta) = \frac{g\sigma}{4k(1-s^2)}sech^2(g\zeta/2). \qquad (56)$$

The following energy is necessary for deformation:

$$W = \frac{1}{2}k(1+s^2)\int\rho^2(\zeta)d\zeta = \frac{1}{24}g^2 J(1+s^2). \qquad (57)$$

Measured from the bottom of the conduction band of a free quasiparticle, the total energy (including that of deformation) transferred by a soliton moving with velocity V is determined by the expression

$$E_s(V) = W + \hbar\omega = E_s(0) + \frac{1}{2}M_{sol}V^2, \qquad (58)$$

in which the energy of a soliton at rest $E_s(0)$ and its effective mass M_{sol} are determined, respectively, by the equalities

$$E_s(0) = \frac{1}{12}g^2 J, \qquad (59)$$

$$M_{sol} = m(1 + \frac{g^2 J}{3a^2 k}). \qquad (60)$$

The soliton mass M_{sol} exceeds the effective mas of a quasiparticle m, as its motion is accompanied by the motion of a local deformation.

The effective potential well where quasiparticles are placed, is determined, in the reference frame ζ, by the expression

$$U = -\sigma\rho(x,t) = -g^2 J \times sech^2(g\zeta/2). \qquad (61)$$

The self-trapped soliton is very stable. The soliton moves with the velocity $V < c_0$, otherwise, the local deformation of the chain will be not able to follow the quasiparticle. Alternatively, the soliton can be stationary.

It is worth emphasizing that the Davydov solitons are conceptually different from the small polarons which are three-dimensional. In fact, the small polarons are practically at rest owing to their large mass.

The bisoliton excitations are discussed separately (Chapter 7 in [14]).

XIII. DISCRETE BREATHERS

In lattices, intrinsic localized modes with internal (envelope) oscillations (see Fig. 11c) are often called *discrete breathers* because an envelope mode or nonlinear wavepacket can be considered as the small amplitude limit of a breather-solution for the continuum sine-Gordon equation and also for other systems in the semi-discrete approximation, where the oscillations (discrete carrier wave) vary rapidly inside the slow (continuous) envelope. In this approximation, discrete breathers are linked to envelope solitons. Contrary to continuous breathers which are known to exist only in some particular systems, discrete breathers are structurally stable as soon as nonlinear oscillators are coupled sufficiently weakly and locally.

In purely harmonic lattices, spatially localized modes can occur only when defects or disorder are present, so that the translational invariance of the underlying lattice is broken. Discrete breathers may be created anywhere in a perfect homogenous nonlinear lattice. As an example, let us consider the behavior of a one-dimensional chain of particles with mass m, bound by massless springs. A similar chain was used in the computer simulations by Fermi, Pasta and Ulam (see above). In this chain, a discrete breather is a nonlinear excitation centered at a lattice site, which involves longitudinal displacements of a few masses. The longitudinal displacements of any two neighboring masses are in antiphase, so that the displacement of the central mass is maximal, and two neighboring masses have smaller, antiphase displacements relatively to the central mass etc. This case corresponds to an *odd parity mode*, however, one may also have an *even parity mode* centered at the midpoint between two masses.

The basic properties of the discrete breather or the *intrinsic localized mode* can be summarized as follows [7]:

 i. It is a time periodic solution localized in space which may occur in one, two or three dimensions.

 ii. It may be centered on any lattice site giving rise to a configurational entropy.

 iii. It extends over a few lattice sites.

 iv. It has an amplitude dependent frequency.

 v. It may be mobile.

Contrary to solitons, discrete breathers do not require integrability for their existence and stability. A particular important condition of breather existence is that all multiples of the fundamental frequency lie outside of the linear excitations spectrum. Discrete breathers are predicted to exist; however, they have not yet been observed experimentally.

XIV. STRUCTURAL PHASE TRANSITIONS

From Chapter 3 we know that the phase diagram of cuprates is very rich on structural phase transitions. What is a structural phase transition? A structural phase transition corresponds to the shifts of the equilibrium positions of the atoms (molecules). They take place owing to the instability of some lattice displacement pattern, which drives the system from some stable high-temperature phase at $T > T_d$ to a different low-temperature lattice configuration at $T < T_d$, where T_d is the critical temperature. The dynamics of such transitions is frequently characterized by a vibrational or phonon mode whose frequency sharply decreases as the temperature approaches the critical temperature T_d from above. As a result, the restoring force corresponding to that displacement pattern softens, and one calls this particular mode a *soft mode*.

At the critical temperature T_d, the lattice displacements become large and *the dynamics is highly nonlinear*. As a consequence, equations describing the structural phase transition become nonlinear. Simulating structural phase transitions in one-dimensional lattice, a model corresponding to a structural phase transition can be presented by a large number of double-well potentials shown in Fig. 15, forming a one-dimensional chain similar to that in Fig. 5. Contrary to the case in Fig. 5, in the latter model, the balls (atoms) cannot jump from one double-well to another, however, being able to change the minima in each double-well potential. Writing down the Hamiltonian, the solution of the obtained nonlinear equation strongly depends on the coupling (spring) strength between nearest-neighbor balls (atoms) and the potential-barrier height inside each double well. In the case of strong coupling between balls (atoms), the equation takes a form of the sine-Gordon equation. The solution of the equation coincides with Eq. (9), having a *tanh* shape and corresponding to a localized kink soliton.

So, the main point of this section is that a structural phase transition can be presented as a localized soliton (domain wall). Owing to preparation, impurity and defects content, the crystal may be in a state of coexistence of two or more structural phases, forming *domains* separated by *walls*.

XV. TUNNELING AND THE SOLITON THEORY

What can we expect from tunneling measurements in a system having solitons?

As discussed in Chapter 2 in [14], a tunneling conductance $dI(V)/dV$ obtained in a superconductor-insulator-normal metal (SIN) junction directly relates to the electron density of states per unit energy interval since voltage V multiplied by e represents energy. All the soliton
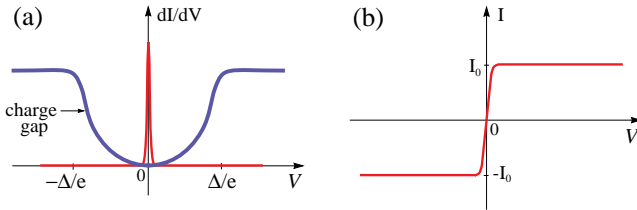
FIG. 23. (a) Same as Fig. 17 but in conductance units: dI/dV vs V (for an SIN junction); and (b) the $I(V)$ characteristic corresponding to the soliton peak in plot (a). The $I(V)$ characteristic of the charge gap is not shown.
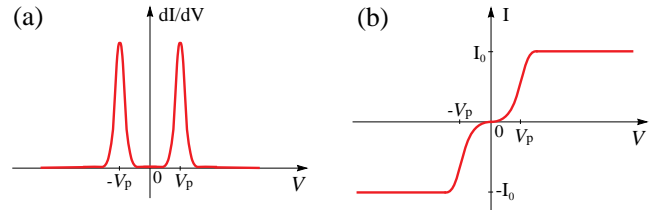

FIG. 24. (a) Same as Fig. 19 but in conductance units: dI/dV vs V (for an SIN junction). The charge gap is not shown, and the width of the conductance peaks is slightly enlarged in comparison with that in Fig. 19. (b) The corresponding $I(V)$ characteristic.

solutions considered above are real-space functions, i.e. functions of x and t. Therefore, before we discuss tunneling measurements in terms of the solitons solutions, we need to transform the solutions from real space into momentum realm.

First, let us *qualitatively* determine the shape of tunneling characteristics caused by solitons. Taking into account that $V = E/e$, Figure 17 is represented in conductance units, dI/dV vs V, in Fig. 23a. Bearing in mind that tunneling current is the sum under the conductance curve, $I(V) = \int \frac{dI(V)}{dV} dV + C$, where C is the constant, the $I(V)$ characteristic of the soliton peak shown in Fig. 23a at zero bias is schematically depicted in Fig. 23b. The constant C is defined by the condition $I(V=0) = 0$.

The same procedure has been done for two polaron peaks shown in Fig. 19: the $dI(V)/dV$ and $I(V)$ characteristics of a polaron are shown in Figs. 24a and 5.24b, respectively.

Let us now *quantitatively* determine the shape of tunneling conductance peak, obtained in a system having topological solitons. In general, the total energy of a soliton consists of the energy of a static soliton and its kinetic energy. For simplicity, consider a static soliton, thus, a soliton with a velocity $v = 0$. The spatial density of states of a topological soliton is determined by $|\psi(x)|^2$, where $\psi(x) = C \times sech(x/d)$ given by Eq. (27). Then, the spectral function $\varphi(k)$ can be found by applying the Fourier transform to $\psi(x)$, where k is the wave number:

$$\varphi(k) = \int_{-\infty}^{\infty} \psi(x) e^{-ikx} dx. \tag{62}$$

Bearing in mind that the Fourier transform of the $sech(\pi x)$ function gives $sech(\pi k)$ [12], then the energy spectrum of a topological soliton is also enveloped by the $sech$ hyperbolic function, centered at some k_0. Then, for $\Delta k = (k - k_0)$, we have $\varphi(\Delta k) = C_1 \times sech(d_1 \Delta k)$, where C_1 and d_1 are constants.

Since $E = \frac{\hbar^2 k^2}{2m}$, where m is the mass, then

$$E(k) - E(k_0) = \Delta E = \frac{\hbar^2 k^2}{2m} - \frac{\hbar^2 k_0^2}{2m} \simeq \frac{\hbar^2 k_0}{m} \Delta k \tag{63}$$

valid in the vicinity of k_0, i.e. for $\Delta k \ll k_0$. Substituting $\Delta k \to \Delta E$, one obtains

$$\varphi(\Delta E) = C_1 \times sech(d_1 \frac{m}{\hbar^2 k_0} \Delta E). \tag{64}$$

Assuming that the soliton energy remains constant, i.e. $k_0 = $ constant, then, the spectral density of states is determined by

$$|\varphi(\Delta E)|^2 = C_1^2 \times sech^2(\Delta E/E_0), \tag{65}$$

where $E_0 = \frac{\hbar^2 k_0}{m d_1}$. Thus, in the vicinity of peak energy, the energy density of states is proportional to $sech^2(\Delta E/E_0)$.

Finally, in SIN tunneling measurements performed in a system having topological solitons, for example, in polyacetylene, one can expect that, near peak bias,

$$\frac{dI(V)}{dV} \simeq A \times sech^2(V/V_0) \tag{66}$$

and

$$I(V) \simeq B \times \tanh(V/V_0), \tag{67}$$

where V is the applied bias, and A, B and V_0 are the constant. In the equations, $\Delta V \to V$ since the peak is centered at zero bias, as shown in Fig. 23a.

By the same token, for the polaron characteristics shown in Fig. 24, one can obtain that, in an SIN junction,

$$\frac{dI(V)}{dV} \simeq A \times \left[sech^2 \left(\frac{V + V_p}{V_0} \right) + sech^2 \left(\frac{V - V_p}{V_0} \right) \right] \tag{68}$$

and

$$I(V) \simeq B \times \left[\tanh \left(\frac{V + V_p}{V_0} \right) + \tanh \left(\frac{V - V_p}{V_0} \right) \right], \tag{69}$$

where V_p is the peak bias, as shown in Fig. 24. The latter equations are valid in the vicinities of $\pm V_p$.

What is interesting is that the results obtained above for a topological soliton are also valid for a static envelope soliton which is schematically shown in Fig. 25a. As
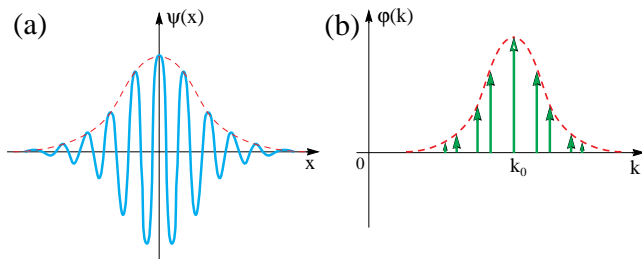
FIG. 25. (a) An envelope soliton in real space, and (b) its energy spectrum, shown schematically.

discussed above, in real space coordinates, the enveloping curve of an envelope soliton has the *sech*-function shape (the dashed curve in Fig. 25a). The energy spectrum of the envelope soliton is schematically presented in Fig. 25b. From the Fourier transform, one can easily obtain that the enveloping curve of energy spectrum of an envelope soliton, shown in Fig. 25b by the dashed line, is also the *sech* hyperbolic function. Hence, for a static envelope soliton, the density-of-state peak of energy spectrum has the $sech^2$-function shape, as for a topological soliton.

Thus, quasiparticle peaks in a conductance obtained in an SIN tunneling junction in a system having either envelope or topological solitons can be fitted by the $sech^2$ hyperbolic function, and the corresponding tunneling $I(V)$ characteristic by the *tanh* hyperbolic function. As a consequence, quasiparticle peaks in a conductance obtained in a superconductor-insulator-superconductor (SIS) tunneling junction have to be fitted by the convolution of the $sech^2$ function with itself [see Eq. (18)]. The convolution cannot be resolved analytically. As shown in Chapter 12 in [14], the $sech^2$- and *tanh*-function fits can be applied also to tunneling spectra obtained in an SIS junction. Therefore, independently from the type of tunneling junction, SIN or SIS, the $sech^2$ function can be used to fit quasiparticle peaks in conductances, and the *tanh* function to fit $I(V)$ characteristics, caused by solitons. However, one has to realize that quasiparticle conductance peaks caused by solitonic states will appear in the "background" originated from other electronic states present in the system.

For a moving soliton, i.e. for $v \neq 0$, the results obtained above are also valid if its velocity v is small.

XVI. MODERN SOLITONS

The modern soliton theory is a very broad area of research not only in different branches of physics but in different branches of science, such as chemistry, biology, medicine, astronomy etc. Practical devices based on the soliton concept, for example, in optics are now a multimillion-dollar industry.

In 1962, that is even before Kruskal and Zabusky's work, Skyrme suggested that elementary particles, for example, protons can be regarded as solitons (in modern usage). He used kink solitons being the exact solutions of the sine-Gordon equation to describe the dynamics of elementary particles. He demonstrated that his solitons behave like fermions. At that time, his ideas were very unpopular. However, rigorous proofs of the equivalence between the sine-Gordon theory and the theory of fermions were given only 15 years later by others.

Attempts to use optical pulses for transmitting information started as soon as good enough quality optical fibers became available. Since even superb quality fibers have dispersion, it is a more or less evident idea to use optical solitons for the transmission of information. The nonlinearity which is normally very small in optical phenomena results in the self focusing of the laser beam. As we already know, the self-focusing phenomena are described by the NLS equation. Thus, the optical soliton is in fact an envelope soliton. In optics, the envelope soliton shown in Fig. 11c is called a *bright soliton* because it corresponds to a pulse of light. There also exists another type of envelope solitons which are called in optics *dark solitons*, because they correspond to a hole in the continuous light (carrier) wave. Using solitons for transmitting the information, the transmission speed of optical fibers is enormous, and can be about 100 Gigabits per second. In addition, soliton communication is more reliable and less expensive.

Solitons are encountered in biological systems in which the nonlinear effects are often the predominant ones [13]. For example, many biological reactions would not occur without large conformational changes which cannot be described, even approximately, as a superposition of the normal modes of the linear theory.

The shape of a nerve pulse was determined more than 100 years ago. The nerve pulse has a bell-like shape and propagates with the velocity of about 100 km/h. The diameter of nerves in mammals is less than 20 microns and, in first approximation, can be considered as one-dimensional. For almost a century, nobody realized that the nerve pulse is the soliton. So, all living creatures including humans are literally stuffed by solitons. Living organisms are mainly organic and, in principle, should be insulants—solitons are what keeps us alive.

The last statement is true in every sense: the blood-pressure pulse seems to be some kind of solitary wave [7]. The muscle contractions are stimulated by solitons [11].

The so-called *Raman effect* is closely related to supplying solitons with additional energy. The essence of the Raman effect is that the spectrum of the scattered (diffused) light is changed by its interaction with the molecules of the medium. Crudely speaking, the incoming wave is modulated by vibrating molecules. These vibrations are excited by the wave, but the frequency of the vibrations depends only on properties of the molecules.

So, I could continue to enumerate different cases and different systems where solitons exist. Nevertheless, I

think that it is already enough information for the reader to understand the concept of the soliton, and to perceive them as real objects because we deal with them every day of our lives.

XVII. NEITHER A WAVE NOR A PARTICLE

At the end, I have a proposal. Solitons are often considered as "new objects of Nature" [5]. It is not true in the global sense. Solitons exist since the existence of the universe. It is true that solitons are "new objects of Nature" *for humans.* However, they existed even before the life began.

Solitons are waves, however, very strange waves. They are not particles, however, they have particle-like properties. They transfer energy, and do it very efficiently. Since the formulation of the relativistic theory, we know that the mass is an equivalent of energy, and relates to it by

$$E = mc^2.$$

From this expression, it is not important if an object has a mass or not: it is an object if it has an ability to transfer (localized) energy.

In my opinion, solitons do not have to be associated neither with waves nor with particles. They have to remain as *solitons.* It is simply a *separate* (and very old) form of the existence of matter. And, they should remain as they are.

I am sure that, in the future, we shall add to the group of *waves, solitons*, and *particles* new names—new forms of the existence of matter. However, it will happens in the future and, right now, let us return to our problem—the mechanism of high-T_c superconductivity in cuprates.

XVIII. APPENDIX: BOOKS RECOMMENDED FOR FURTHER READING

- M. Remoissenet, *Waves Called Solitons* (Springer-Verlag, Berlin, 1999).
- A. S. Davydov, *Solitons in Molecular Systems* (Kluwer Academic, Dordrecht, 1991).
- A. T. Filippov, *The Versatile Soliton* (Birkhäuser, Boston, 2000).
- G. Eilenberger, *Solitons* (Springer, New-York, 1981).
- F. K. Kneubühl, *Oscillations and Waves* (Springer, Berlin, 1997).
- *Solitons and Condensed Matter Physics*, A. R. Bishop and T. Schneider, (ed.) (Springer, Berlin, 1978).
- *Nonlinearity in Condensed Matter*, A. R. Bishop, D. K. Cambell, P. Kumar, and S. E. Trullinger, (ed.) (Springer, Berlin, 1987).
- M. Lakshmanan, *Solitons* (Springer, Berlin, 1988).

[1] J. S. Russell, *Report on Waves*, in *Rep. 14th Meet. British Assoc. Adv. Sci.* (John Murray, 1844) p. 311.

[2] D. J. Korteweg and G. de Vries, *On the Change of Form of Long Waves Advancing in a Rectangular Canal, and on a New Type of Long Stationary Waves*, Phil. Mag. **39**, 442 (1895).

[3] E. Fermi, J. Pasta, and S. Ulam, *Studies of Nonlinear Problems* (Los Alamos National Laboratory, Los Alamos, 1955) Report No. LA1940.

[4] N. J. Zabusky and M. D. Kruskal, *Phys. Rev. Lett.* **15**, 240 (1965).

[5] A. T. Filippov, *The Versatile Soliton* (Birkhäuser, Boston, 2000).

[6] Yu. I. Frenkel and T. A. Kontorova, *J. Phys. Moscow* **1**, 137 (1939).

[7] M. Remoissenet, *Waves Called Solitons* (Springer-Verlag, Berlin, 1999).

[8] W. P. Su, J. R. Schrieffer, and A. J. Heeger, *Phys. Rev. B* **22**, 2099 (1980).

[9] E. J. Mele and M. J. Rice, *Phys. Rev. B* **23**, 5397 (1981).

[10] A. S. Davydov, *Phys. Rep.* **190**, 191 (1990).

[11] A. S. Davydov, *Solitons in Molecular Systems* (Kluwer Academic, Dordrecht, 1991).

[12] G. A. Cambell and R. M. Foster, *Fourier Integrals for Practical Applications* (D. Van Nostrand Company, New York, 1951) p. 73.

[13] M. Peyrard, (ed.), *Nonlinear Excitations in Biomolecules* (Springer-Verlag, Berlin, 1995).

[14] A. Mourachkine, *High-Temperature Superconductivity: The Nonlinear Mechanism and Tunneling Measurements* (Kluwer Academic, Dordrecht, 2002).